

Received January 7, 2019, accepted January 22, 2019, date of publication February 25, 2019, date of current version April 1, 2019.

Digital Object Identifier 10.1109/ACCESS.2019.2900986

# A Low Error Rate BCH-Based Encoder-Decoder Approach for Electromagnetic Measurement While Drilling System

CHENG ZHANG<sup>1,2,3</sup>, HAOBIN DONG<sup>1,2,3</sup>, JIAHAO WANG<sup>2,4</sup>, JIAN GE<sup>1,2,3</sup>,  
HUAN LIU<sup>1,2,3</sup>, (Member, IEEE), ZHIWEN YUAN<sup>3</sup>,  
JUN ZHU<sup>3</sup>, AND HAIYANG ZHANG<sup>3</sup>

<sup>1</sup>School of Automation, China University of Geosciences, Wuhan 430074, China

<sup>2</sup>Hubei Key Laboratory of Advanced Control and Intelligent Automation for Complex Systems, Wuhan 430074, China

<sup>3</sup>Science and Technology on Near-Surface Detection Laboratory, Wuxi 214035, China

<sup>4</sup>School of Mechanical Engineering and Electronic Information, China University of Geosciences, Wuhan 430074, China

Corresponding author: Haobin Dong (donghb@cug.edu.cn) and Huan Liu (huan.liu@cug.edu.cn)

This work was supported in part by the National Natural Science Foundation of China under Grant 41474158 and Grant 41874212, in part by the Foundation of Qingdao National Laboratory for Marine Science and Technology under Grant QNLM2016ORP0201, in part by the National Key Scientific Instrument and Equipment Development Project of China under Grant 2014YQ100817, in part by the Foundation of Science and Technology on Near-Surface Detection Laboratory under Grant 6142414180913, Grant TCGZ2016A005, Grant 614241409040218, and Grant 614241409041217, in part by the Chinese Postdoctoral Science Foundation under Grant 2016M592410, and in part by the 111 project under Grant B17040.

**ABSTRACT** In practical applications of electromagnetic measurement while drilling (EM-MWD) in the underground coal mine, the signal-to-noise ratio (SNR) of a receiver cannot always meet the requirements of reliable communication conditions due to the earth attenuation, interfering signal from the well site, and so on. Aimed to solve these problems, this paper presents a low error rate Bose–Chaudhuri–Hocquenghem (BCH)-based encoder–decoder technology for EM-MWD. First, this paper studies the relationship among the BCH encoding error performance and the decoding method, the source length, and other factors through simulation; then, we obtain an optimal length of BCH code for EM-MWD through analyzing the bit error performance of hard-decision decoding and soft-decision decoding with different lengths of BCH code. Finally, we compare the proposed algorithm with the conventional binary phase-shift keying (BPSK) approach in the actual environment. The results show that the proposed algorithm can reduce the bit error rate by about ten times at a lower SNR, achieving a reliable communication condition when the SNR of a received signal is reduced. It demonstrates the effectiveness of the proposed BCH encoder and the decoder algorithm based on BPSK for EM-MWD.

**INDEX TERMS** EM-MWD system, BPSK, BCH coding, optimized coding techniques.

## I. INTRODUCTION

During the process of special drilling, the keys to ensuring drilling quality are rapid, efficient and accurate control of well trajectory. In practical applications of measurement while drilling (MWD), transforming the sensor data from the drill bit to the surface in real-time is a critical factor that can reduce downtime and improve work efficiency [1], [2]. The wireless MWD system is a technology that can measure various parameters continuously in real time while drilling [3], [4]. Up to now, wireless MWD has three kinds of ways: mud pulse transmission, electromagnetic transmission, and acoustic transmission. The advantage of mud pulse trans-

mission is that there is no need for insulated cables and special drill rods, but its transfer rate is relative slow, and it contains less information. The acoustic transmission is mainly adopted in horizontal wells due to the signal attenuates rapidly, it has a high data transfer rate and does not require mud circulation. But it can only transmit few information. Moreover, there is a high degree of interference when it is transmitted through the formation. EM-MWD (Electromagnetic Measurement While Drilling) does not need the mud as a signal carrier and requires less for drilling fluids or drilling pumps, it has a better data transfer capability and a better adaptability to underbalanced wells [5], [6].

Figure 1 shows the schematic of the EM-MWD system, which mounts an electromagnetic launcher in the downhole transmitter and generates a low frequency current by exciting

The associate editor coordinating the review of this manuscript and approving it for publication was Guido Lombardi.

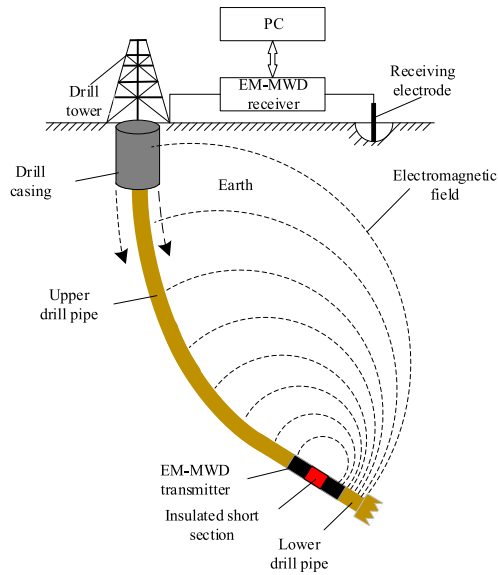


FIGURE 1. EM-MWD system diagram.

a conductor drill pipe in the formation. Thus, an electromagnetic field signal around the ground layer is formed, and the surface receiver uses the drill pipe and the electrode as a set of receiving antennas to acquire signals using geodesic method. During drilling, the dielectric short section divides the drill pipe into two parts which constitutes two asymmetric dipoles. The electromagnetic wave signal is applied to two asymmetric dipoles. Hence, the drill pipe, the borehole wall, and the formation between them form the transmission path for the EM-MWD system. During the transmission of electromagnetic wave signals, the signal attenuated severely due to the influence of formation resistivity [7]. Therefore, the distance and rate of electromagnetic signal transmission are limited. The operating frequency of the electromagnetic signal can be decreased to increase the transmission distance [8]. However, the data transmission rate would be decreased. In addition, due to the limited conductivity of the drill pipe, the attenuation constant has nothing to do with the operating frequency while the electromagnetic signal frequency reduced to several hertz. Hence, we cannot increase the signal transmission distance effectively by reducing the signal frequency [9]. Furthermore, the working frequency is generally less than 100Hz when the signal is transmitted to several kilometers [10], [11].

Currently, in the field of the wireless MWD, most of the mud MWD systems use pulse modulation as the modulation method [12], such as on-off keying (OOK), pulse position modulation (PPM), pulse interval modulation (PIM) and so on [13], [14]. In addition, Manchester code is also widely used in mud MWD [15]. These signals have abundant low-frequency components, we cannot transmit such signals in actual EM-MWD channels directly because of the band-pass characteristics in the channels unless they are modulated by carrier modulation [16], [17]. To solve this problem, Haliburton proposed phase shift keying (PSK) [18],

and Sinopec uses binary phase shift keying in the prototype named CEM-1 [19].

Electromagnetic signal would be attenuated severely while transmitted from the well bottom to the surface. Due to the influence of the drilling construction site, the received electromagnetic signal could be mixed with the power-line interference near the wellhead and the natural potential signal, which will lead to error code and low data transmission accuracy [20]. Aimed to improve the reliability of data transmission, some commercial corporation proposed to adopt channel error correction coding technology in the EM-MWD system, to guarantee the SNR of signal bit can achieve a reliable communication condition. Baker Hughes uses the cyclic redundancy check-16 (CRC-16) as the internal code and the convolutional code as the external code for the image data of boreholes. The internal code is cascaded with the external code, which has both error detection and error correction capabilities [21], [22]. Shell proposes to use Turbo code or low density parity check code (LDPC) in wellbore communication [23]. However, for technical confidentiality considerations, the details of channel coding method for EM-MWD are not available, therefore, we cannot know some of the key technologies.

Nowadays, a commonly used and accepted decoding method namely BCH has shown its effectiveness in many fields, such as wireless communication applications, NAND flash memory applications, etc [24]–[26]. However, the details on how to use BCH in MWD system is not available, and there are few researches on the relation among EM-MWD system and BCH coding error performance, decoding method and source length. Moreover, the optimal BCH code length to the EM-MWD channel is not discussed.

Aimed to solve the problems mentioned before, this paper presents a BCH encoder and decoder technology based on binary phase shift keying (BPSK) for EM-MWD. The contributions are as follows:

1. Considering the characteristics of the EM-MWD channel and the transmission data, we study the relationship between BCH encoding error performance and decoding method, source length and other factors through simulation;
2. We obtain an optimal length of BCH code for EM-MWD through analyzing the bit error performance of hard-decision decoding and soft-decision decoding with different lengths of BCH code;
3. We compare the proposed algorithm with conventional BPSK approach in the actual environment to prove the effectiveness of the proposed method.

## II. BCH CODE DESIGN OF EM-MWD SYSTEM

### A. BINARY PHASE SHIFT KEYING

In practical applications of EM-MWD, the data is not suitable for the transmission of the terrestrial channel after being encoded and must be modulated by the carrier before being transmitted. The commonly used modulation methods are generally divided into three types: amplitude

modulation (e.g., amplitude shift keying), frequency modulation

(e.g., frequency shift keying) and phase modulation (e.g., phase shift keying). Compared with other methods, the phase modulation has the following advantages including moderate spectrum utilization, good anti-interference, and it is more suitable for EM-MWD communication system with limited power and bandwidth.

PSK is a kind of modulation using carrier phase variation to transfer digital information, while BPSK is a binary carrier phase modulation method. To distinguish the phase of signals representing “0” and “1”,  $0^\circ$  and  $180^\circ$  are usually selected to represent the above two different kinds of information, respectively [27].

Assuming that  $A_c$  is the amplitude of the carrier signal and  $f_c$  is the carrier signal frequency. The transmission period of binary information bit is  $T_b$ , thus the transmission rate  $R_b = 1/T_b$ . In addition, the bilateral power spectral density of additive white Gaussian noise (AWGN) channel is  $N_0/2$  W/Hz. If the amplitude of the transmitted pulse sequence  $\{a_n\}$  is a binary random variable with  $a_n \in \{1, -1\}$ , the BPSK signal can be expressed as:

$$x_{BPSK}(t) = A_c \sum_{n=-\infty}^{\infty} a_n \prod [(t - nT_b)/T_b] \cos(2\pi f_c t), \quad (1)$$

where, the rectangular pulse can be written as:

$$\prod [(t - nT_b)/T_b] = \begin{cases} 1, & (n - \frac{1}{2})T_b \leq t \leq (n + \frac{1}{2})T_b \\ 0, & \text{other} \end{cases}. \quad (2)$$

Generally, the power spectral density of BPSK signal can be written as:

$$G_{BPSK}(f) = \frac{E_b}{2} \left\{ \text{sinc}^2 [(f - f_c)/R_b] + \text{sinc}^2 [(f + f_c)/R_b] \right\}, \quad (3)$$

where, the average energy per bit  $E_b = A_c^2 T_b/2$ .

The power spectrum of the BPSK signal only contains the continuous spectrum. Its spectral characteristics are mainly determined by the baseband symbol sequence and the baseband signal's waveform. In the BPSK modulation process, the signal bandwidth will be expanded to double the original baseband signal bandwidth. Hence, the spectral efficiency is only half times of the baseband transmission system.

## B. BCH CODE

The BCH code is an abbreviation taken from Bose, Ray-Chaudhuri and Hocquenghem, which is a cyclic code that can correct multiple random errors. Its error correction capability is very strong, and the performance is very close to the theoretical value, especially in the short and medium code length. It also has the advantages of easy construction and simple coding. Furthermore, it has a strict algebraic structure and plays an important role in coding theory [27].

For any positive integer  $m \geq 3$  and  $t \leq 2^{m-1}$ , there is a binary BCH code with a code length of  $2^m - 1$  with a minimum

distance of at least  $2t + 1$  and at most  $mt$  parity bits. This BCH code can correct  $t$  random errors within the span of  $2^{m-1}$  transmission code bits. We use  $(n, k)$  to represent the BCH code, where  $n$  is the code length after encoding and  $k$  is the number of useful information bits before encoding.

The encoding process can be written in the form of a polynomial, the message vector is known, and the message polynomial can be obtained as:

$$m(x) = m_0 + m_1x + \dots + m_{k-1}x^{k-1}. \quad (4)$$

Then, we need to shift the message matrix as:

$$x^{n-k}m(x) = m_0x^{n-k} + m_1x^{n-k+1} + \dots + m_{k-1}x^{n-1}. \quad (5)$$

Divide the message polynomial after shifting by the generator polynomial as:

$$x^{n-k}m(x) = a(x)g(x) + b(x), \quad (6)$$

where,  $a(x)$  and  $b(x)$  are the quotient and the remainder, respectively. Generally,  $b(x)$  can be written as:

$$b(x) = b_0 + b_1x + b_2x^2 + \dots + b_{n-k+1}x^{n-k+1}. \quad (7)$$

In this case, the codeword polynomial used to transmit is the sum of the message polynomial and the remainder:

$$\begin{aligned} c(x) &= x^{n-k}m(x) + b(x) = a(x)g(x) \\ &= m_0x^{n-k} + m_1x^{n-k+1} + \dots + m_{k-1}x^{n-1} \\ &\quad + b_0 + b_1x + b_2x^2 + \dots + b_{n-k+1}x^{n-k+1}. \end{aligned} \quad (8)$$

The overall system model is shown in Figure 2, which is consist of a transmitter and a receiver. The function of the transmitter is to encode and modulate the data measured by the sensors and transmits it through the antenna. The receiver receives the signal through the electrode, decoding it after filtering and amplifying, and then transmits the data to the PC.

The steps of BCH encoding can be summarized as:

*Step 1:* Multiply the message  $m(x)$  by  $x^{n-k}$ . This multiplication is equivalent to shifting the message bits by  $n-k$  positions to the right;

*Step 2:* Divide the  $x^{n-k}m(x)$  by the generator polynomial  $g(x)$  to compute the remainder  $b(x)$ . The remainder stands for the parity check digits;

*Step 3:* Add the computed remainder  $b(x)$  to  $x^{n-k}m(x)$  to obtain the code-word polynomial  $c(x)$ .

The general decoding algorithm block diagram is shown in Figure 3. The concrete steps are as follows:

*Step 1:* Calculate the syndrome  $s$  of  $R(x)$ ;

*Step 2:* Calculate the error location polynomial  $\sigma$  through the syndrome  $s$ ;

*Step 3:* Calculate the root of the error location polynomial, and then determine where the errors occur;

*Step 4:* Calculate the value of the error location  $Y_i$ , and then complete the error correction combined with the location of the error.

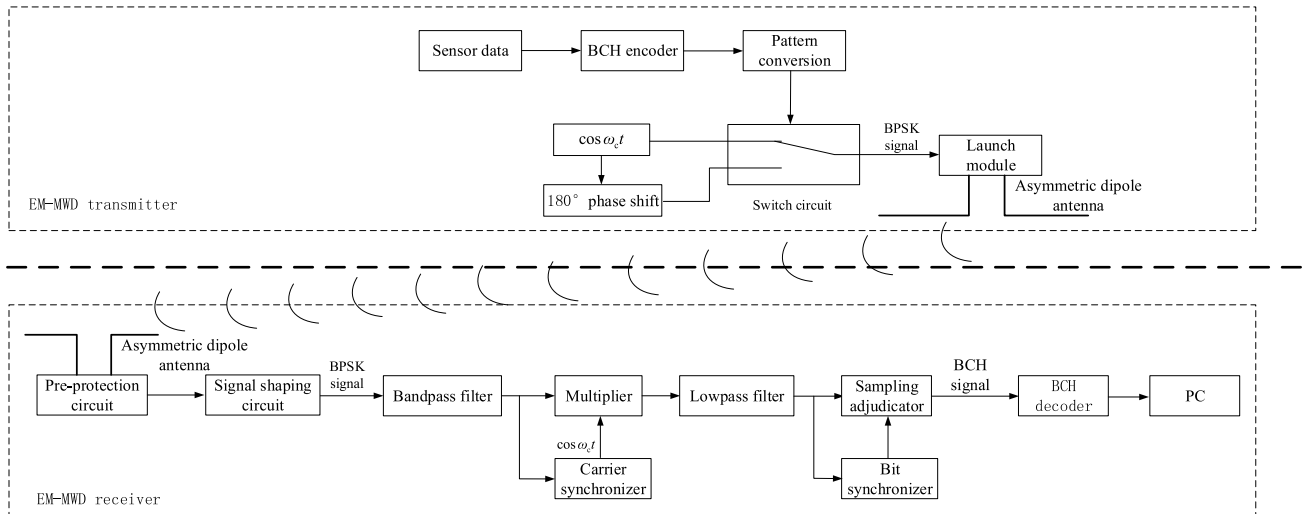


FIGURE 2. General communication model of EM-MWD system.

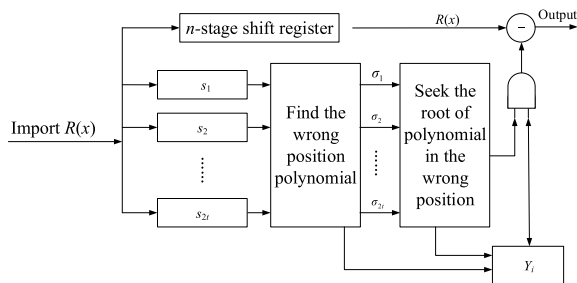


FIGURE 3. BCH code decoding block diagram.

### III. THE SIMULATION ANALYSIS OF BCH CODE

#### A. SENDING DATA CHARACTERISTICS OF MWD

In practical drilling process, the data could be divided into two launch modes to improve the work efficiency. During drilling, the system only sends a tool face angle (short data, 10 bits) used to adjust the drill pipe gesture and sends all data (long data, 94 bits) when stop drilling, as shown in Table 1. Both long data and short data are encapsulated into different lengths of data frames. Compared with the way of splitting long data into several short data, this way can reduce the data of start flag and end flag or other redundant information, which will help us increase the sending efficiency.

Since  $n = 2^m - 1$  and  $m \geq 3$  the length of  $n$  can be 7, 15, 31, 63, 127, 255, etc., in which the excessive  $n$  will cause too much redundant data. Therefore, for short data of 10 bits, we choose  $n = 15$  and  $n = 31$  for comparative analysis. For long data of 94 bits, we choose  $n = 127$  and  $n = 255$  for comparison. We select the appropriate BCH code for analysis based on the binary original BCH code table [28]. For short data, when  $n = 15$  and  $k \geq 10$ , only one BCH code (15,11) satisfies the requirement, the encoding efficiency is 73.3%. When  $n = 31$ , we choose three sets of BCH codes with different decoding efficiencies for comparison, which are (31,11), (31,16) and (31,26), and their encoding efficiency

TABLE 1. Measurement parameters of EM-MWD system.

Dip	10bits
Azimuth	10bits
Tool Face Angle	10bits
Temperature	10bits
Pressure	10bits
Vector Sum of Gravity Field	16bits
Magnetic Field Intensity	16bits
Battery Voltage of Sensor	6bits
Voltage of Battery Cartridge	6bits

are 35.5%, 51.6% and 83.9%, respectively. Likewise, for long data, when  $n = 127$  and  $k \geq 94$ , we choose (127,99), (127,113) and (127,120) for comparison, and their encoding efficiency are 78.0%, 89.0% and 94.5%, respectively. When  $n = 255$ , we choose (255,99), and the encoding efficiency is 38.8%.

#### B. ELECTROMAGNETIC COMMUNICATION CHANNEL CHARACTERISTICS OF MWD

According to literatures [9], [29], [30], the attenuation characteristics of electromagnetic signals during channel transmission are studied, and the following conclusions are obtained. (1) The electromagnetic signal is seriously attenuated by the ground layer, and the formation resistivity suitable for EM-MWD is usually  $2 \sim 2000 \Omega \cdot m$ ; (2) If the transmission distance of the EM-MWD signal is up to a kilometer, the operating frequency of the electromagnetic signal should be no more than 100Hz. Hence, in this paper, we assume that

the uniform formation resistivity  $\rho$  is  $2\sim 2000\Omega\cdot m$  around the borehole, the relative permittivity  $\epsilon_r$  does not exceed 200, and the maximum operating frequency of an electromagnetic signal is 100Hz. According to the classical electromagnetic theory, there is:

$$\frac{\text{Conducted current}}{\text{Displacement current}} = \frac{\sigma}{\omega\epsilon} = \frac{1}{2\pi f \rho \epsilon_r \epsilon_0}, \quad (9)$$

where,  $\sigma$  is the conductivity of the formation,  $f$  is the operating frequency of the electromagnetic signal, and the free space permittivity  $\epsilon_0 = 8.85 \times 10^{-12} \text{F/m}$ . Then, there is:

$$\frac{\sigma}{\omega\epsilon} > \frac{1}{2\pi \times 100 \times 2000 \times 200 \times 8.85 \times 10^{-12}} \approx 449. \quad (10)$$

It can be seen that when the electromagnetic signal propagates in a uniform layer, the conduction current is much larger than the displacement current. Hence, in the EM-MWD communication system modeling, we can regard the EM-MWD electromagnetic communication channel as a Gaussian white noise AWGN channel and does not consider the shadow fading and multipath fading.

### C. HARD DECISION DECODING

The error probability is the main index to measure the reliability of the data communication system. This paper mainly discusses the codeword error probability  $P_e$  and the bit error probability  $P_b$ . Codeword error probability refers to the proportion of the number of error words that occur in the total number of transmitted characters. Bit error probability refers to the proportion of the number of bits in error that occur in the total number of transmitted bits. Hard decision decoding refers to the demodulator makes a judgment on the received signal to output 0 or 1, based on its decision threshold. Soft decision decoding means that the demodulator outputs analog data directly without decision, or demodulator outputs waveform for multi-level (not a simple two-level 0 and 1), and then sends to the decoder. The difference from the hard decision decoding is that the output of the encoder channel is a "soft message" without adjudicated.

Based on the characteristics of EM-MWD communication channel analyzed before, we regard the EM-MWD communication channel as an AWGN channel when establishing a downhole EM-MWD channel coding model for a coal mine.

If a hard decision decoding is taken, the codeword error probability of BCH code is shown as follows while we use coherent BPSK demodulation on a binary symmetric channel:

$$\begin{aligned} P_e &= \sum_{m=t+1}^n \binom{n}{m} p^m (1-p)^{n-m} \\ &= 1 - \sum_{m=0}^t \binom{n}{m} p^m (1-p)^{n-m}, \end{aligned} \quad (11)$$

Similarly, the bit error probability of BCH code is:

$$P_b \approx \frac{1}{n} \sum_{m=t+1}^n m \binom{n}{m} p^m (1-p)^{n-m}, \quad (12)$$

where,  $p$  is the symbol error probability of binary symmetry channel.

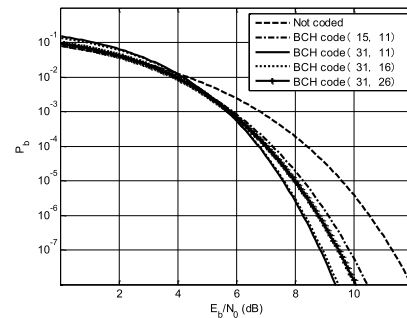


FIGURE 4. BCH code bit error probability of short data in hard decision decoding.

According to the characteristics of downhole EM-MWD data transmission including 10bits short data and 94bits long data, we analyze the error performance of different length BCH code  $(n,k)$  in the electromagnetic communication channel. The short data are BCH code  $(15,11)$ , BCH code  $(31,11)$ , BCH code  $(31,16)$  and BCH code  $(31,26)$ . The long data are BCH code  $(127,99)$ , BCH code  $(127,113)$ , BCH code  $(127,120)$ , and BCH code  $(255,99)$ . The relationship between their bit error probability and the SNR per bit  $E_b/N_0$  for short data is shown in Figure 4. It shows the SNR of the BCH code  $(31,11)$  is slightly lower than that of the BCH code  $(31,16)$  with a bit error probability of  $10^{-6}$ , and both are better than the BCH code  $(15,11)$  and BCH code  $(31,26)$ . In general engineering applications, the bit error probability of  $10^{-6}$  is sufficient to meet the high-performance requirements of communication systems. Figure 5 shows the relationship between the bit error probability and the SNR per bit  $E_b/N_0$  for long data. It indicates that when the bit error probability is  $10^{-6}$ , the order from good to bad are BCH code  $(255,99)$ , BCH code  $(127,99)$ , BCH code  $(127,113)$ , BCH code  $(127,120)$ .

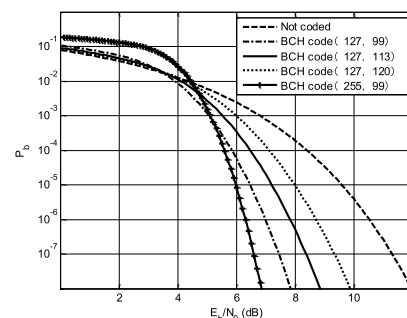


FIGURE 5. BCH code bit error probability of long data in hard decision decoding.

The relationship between the codeword error probability and the SNR per bit  $E_b/N_0$  for short data is shown in Figure 6.



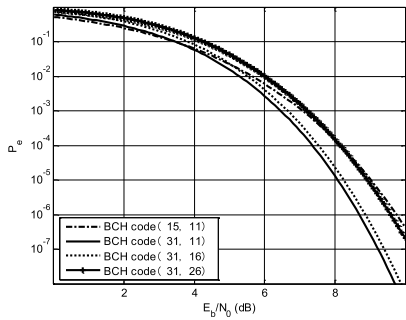


FIGURE 6. Codeword error probability of BCH code for short data in hard decision decoding.

We observe that the SNR of the BCH code (31,11) is slightly lower than that of the BCH code (31,16) with a bit error probability of  $10^{-6}$ , and both are better than the BCH code (15,11) and BCH code (31,26). It is easy to know that BCH code (31,11) has a slightly higher performance because it has more error correction bits than BCH code (31,16). However, BCH code (31,16) has a higher encoding efficiency. Figure 7 shows the relationship between the codeword error probability and the SNR per bit  $E_b/N_0$  for long data. Likewise, when the bit error probability is  $10^{-6}$ , the order from good to bad are BCH code (255,99), BCH code (127,99), BCH code (127,113), BCH code (127,120). Through the above comparisons, we find that the BCH code (255,99) performs better, but it adds too much redundant data, so we think BCH code (127,99) is a better choice for long data.

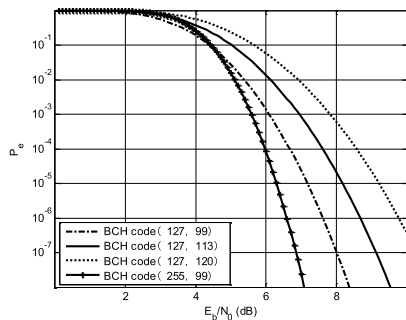


FIGURE 7. Codeword error probability of BCH code for long data in hard decision decoding.

D. SOFT DECISION DECODING

For 10bits short data, if BCH code coding scheme is adopted, BCH code (31,16) has higher coding efficiency, and the following is the soft decision decoding performance of BCH code (31,16).

If the soft decision decoding is adopted, there are two representations on the upper boundary of the codeword error probability while we use coherent BPSK demodulation on a binary symmetric channel:

$$P_e \leq (A(Z) - 1), \tag{13}$$

and

$$P_e \leq e^{-E_b/N_0 \left( R_c d_{min} - \frac{k \ln 2}{E_b/N_0} \right)}, \tag{14}$$

where,  $A(Z)$  is the weight enumeration function,  $Z = \exp(-R_c E_b/N_0)$ , the code rate  $R_c = k/(2^m - 1)$ , and  $d_{min}$  is the minimum distance of the code, which is the minimum of all possible distance between codewords.

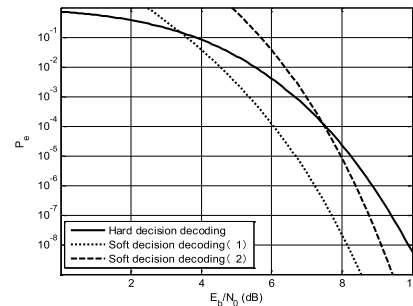


FIGURE 8. Soft decision decoding and hard decision decoding of BCH code (31,16).

Figure 8 shows the comparison between the upper bounds of the codeword error probability of the soft decision decoding and the codeword error probability of the hard decision decoding. We observe that there is a difference of 1~2dB between upper bound 1 of soft decision and upper bound 2 of soft decision. When the codeword error probability is  $10^{-6}$ , the SNR of soft decision decoding is lower than that of hard decision decoding.

To be specific, the Simulink was used to build a BCH code simulation model based on the AWGN channel, coherent BPSK demodulation and soft decision decoding. The BCH code (31,16) and BCH code (127,99) with higher coding efficiency were selected to compare with the uncoded BPSK communication system. As shown in Figure 9, at a bit error rate of  $10^{-6}$ , the BCH code (31,16) has a coding gain of approximately 5.5dB compared with the uncoded BPSK. Similarly, Figure 10 shows that when the bit error rate is  $10^{-6}$ , the BCH code (127,99) has a coding gain of about 4.7dB compared with the uncoded BPSK. This implies that, under the condition of the same bit error rate, the proposed BPSK-based BCH coding technology has lower requirements on the system SNR. In other words, when the SNR is relatively low, it can still maintain a relatively low error rate.

When the bit error probability is  $10^{-6}$ , we compare the bit error probability performance of BCH code (15,11), BCH code (31,11), BCH code (31,16), BCH code (31,26), BCH code (127,99), BCH code (127,113), BCH code (127,120) and BCH code (255,99) through theoretical calculation and simulation, and the results are shown in Table 2. Through analyzing the length of different BCH code's performance, we can get the following conclusions:

- 1) BCH code (31,16) is more suitable for EM-MWD short data transmission than BCH code (15,11), BCH code (31,11) and BCH code (31,26). When the bit error

TABLE 2. Bit error probability performance comparisons of EIGHT length BCH codes.

BCH Code	$N$	$K$	Code Length of Error Correction ( $T$ )	SNR (hard decision decoding)	SNR (soft decision decoding)	Bandwidth Expansion
(15,11)	15	11	1	9.1dB	—	36.7%
(31,11)	31	11	5	8.4dB	—	181.8%
(31,16)	31	16	3	8.3dB	5.2dB	93.8%
(31,26)	31	26	1	8.8dB	—	19.2%
(127,99)	127	99	4	7.0dB	5.9dB	28.3%
(127,113)	127	113	2	7.8dB	—	12.4%
(127,120)	127	120	1	8.7dB	—	5.8%
(255,99)	255	99	23	6.3dB	—	157.6%

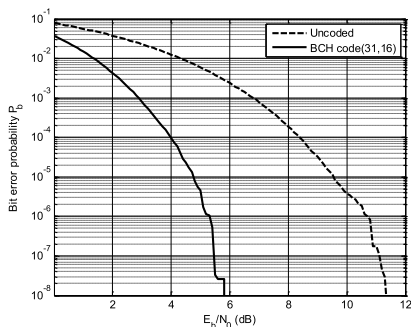


FIGURE 9. The simulation bit error probability performance of BCH code (31,16) in soft decision decoding.

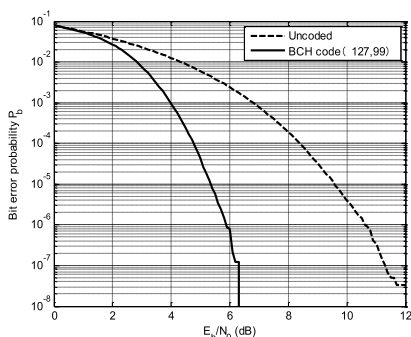


FIGURE 10. The bit error probability performance of BCH code (127,99) in soft decision decoding.

probability is  $10^{-6}$ , the SNR of soft decision decoding is 5.2dB, which is better than the 8.3dB of hard decision decoding. With soft decision decoding, the coding gain of the BCH code (31,16) is 5.5dB and the bandwidth extension is 93.8%;

- 2) BCH code (127,99) is more suitable for EM-MWD short data transmission than BCH code (127,113), BCH code (127,120) and BCH code (255,99). When the bit error probability is  $10^{-6}$ , the SNR of soft decision decoding is 5.9dB, which is better than the 7.0dB of hard decision decoding. With soft decision decoding, the coding gain of the BCH code (127,99) is 4.7dB and the bandwidth extension is 28.3%;
- 3) When the bit error rate is  $10^{-6}$ , the coding gain of the BCH code (31,16) is about 5.5dB compared to the uncoded BPSK, and the coding gain of the BCH code (127,99) is about 4.7dB compared to the uncoded BPSK.

#### IV. EXPERIMENTAL RESULTS AND DISCUSSION

To verify the effectiveness of BCH coding in practical applications, we conduct experiments using an EM-MWD prototype and compare the short data BCH code (31,16) with the uncoded BPSK system. A wire is used to simulate the drill pipe, and the upper transmitter electrode is directly connected with the receive electrode of the receiver. The signal from the transmitter is connected with the lower emitter electrode via a high-power adjustable resistor  $R$  and enters the earth. It is transmitted through the ground as a transmission medium to the other electrode of the receiver. Through the resistor  $R$ , we can change the transmitter’s emission current to control the peak-to-peak of the received signal. The test diagram is shown in Figure 11.

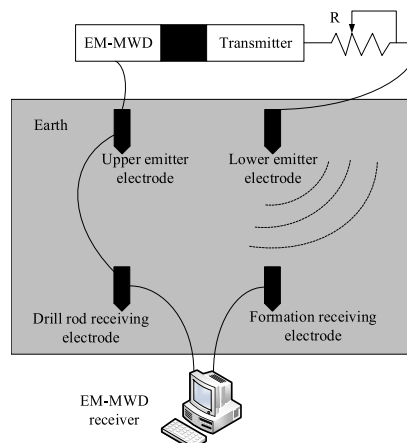


FIGURE 11. Schematic diagram of the test.

##### A. INDOOR TESTING

The coded signal is output through the transmitting circuit, and the waveform is observed at the receiver. To facilitate observation, the transmission signal is fixed at 0101 0101 0101 0101, after BCH encoding, the signal becomes 0101 0101 0101 0101 1010 0000 0110 000. The first 16 bits are information bits and the last 15 bits are check bits. Figure 12 shows the signal processing flow of a short data format. The receiver acquires waveforms, filters and amplifies them, then multiplies with the carrier signal, and then decodes after passing through a low-pass filter.

A series resistor is used to attenuate the signal at the transmitter, the test results are shown in Table 3. When the

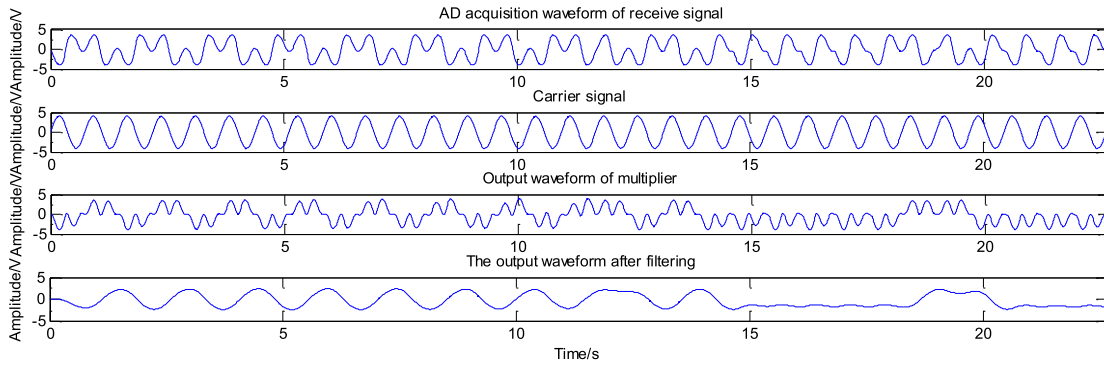


FIGURE 12. Signal processing flow chart.

TABLE 3. Test result of receive signal indoor.

Peak-to-peak of the received signal (mV)	Bit error rate (BPSK)	Bit error rate (BPSK+BCH)
8000	0	0
1000	0	0
400	0	0
...	...	...
1	0	0
0.4	0.0021	0
0.1	0.0633	0.01

signal is attenuated to 0.4mV, a bit error occurs in the BPSK data without BCH encoding. While the signal is attenuated to 0.1mV, the bit error occurs in the BPSK based BCH coding modulation system, and its bit error rate is much lower than the other system. This demonstrates that the effective of BPSK-based BCH coding and modulation technology is better than that of BPSK system without BCH coding. Due to the hardware filter performance of the EM-MWD system and the limitation of the decoding performance of the MCU, the BER performance in the actual test is generally lower than the BER performance in the simulation experiment.

**B. OUTDOOR TESTING**

Aiming to further verify the effectiveness of the proposed technique, we conducted an outdoor experiment for simulating the practical underground environment. The transmitter is installed in the drill pipe and we use a pump switch to control the launch. The interference noise strength on the experimental site is about 0.3V. As shown in Figure 13, During drilling, the insulation short section divides the drill pipe into two parts of insulation which constitutes two asymmetric dipoles. The electromagnetic wave signal is applied to two asymmetric dipoles. The upper drill pipe is connected to an electrode of the receiver and the lower one connected to ground. In this experiment, we used a signal-core cable to simulate the upper drill pipe and connect it to one of the electrodes of the receiver. The transmitted signal current is injected into the water through the upper and lower portions of the transmitter, and the electromagnetic communication signal is transmitted to the formation receiving electrode via the earth’s surface, and a signal is obtained between the

drill pipe receiving electrode and the formation receiving electrode. In this case, the received signal still includes natural potential, electromagnetic communication signal, power-line interference, etc. The maximum distance between the transmitter and the receiver is about 300m.



FIGURE 13. Experimental diagram.

TABLE 4. Outdoor test result.

Peak-to-peak of the received signal (mV)	Signal to noise ratio (dB)	Bit error rate (BPSK)	Bit error rate (BPSK+BCH)
1500	13.98	0	0
500	4.44	0	0
200	-3.52	0	0
100	-9.54	0	0
...	...	...	...
15	-26.02	0	0
8	-31.48	0.0026	0
4	-37.50	0.0108	0.0011
2	-53.52	0.1123	0.0121

Table 4 shows the test results. Due to the hardware circuit limitations and strong noise interference in the real test environment, the system’s BER performance is further degraded. When the signal is attenuated to 8mV, BPSK data errors occur, and the BCH code (31,16) error rate is still 0 because it can correct 3 bits errors in the encoded data transmitted in the channel. When the signal amplitude is



reduced to 2mV, compared with BPSK without BCH coding, the BPSK-based BCH coding and modulation technology can reduce the decoding error rate by about 10 times, reducing the system's bit error rate effectively, which demonstrates that the proposed method is practicality and reliability in high-noise background. In the actual test, the bit error rate result is quite different from the simulation result, due to the uncontrollable external environment, power noise (50 or 60Hz), natural potential, and the influence of the prototype's electrical noise, etc. However, the trends of the two test results are consistent. In terms of the actual situation, reliable communication conditions can still be achieved, and the received data can be stabilized when the SNR is relatively low.

## V. CONCLUSION

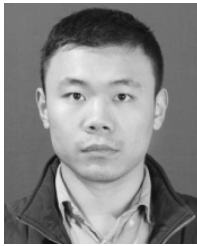
In this study, we propose a BCH encoder and decoder technology based on BPSK for EM-MWD. First, we get the suitable length for the EM-MWD channel by studying the relationship among BCH encoding error performance and decoding method, source length and other factors through simulation. BCH code (31,16) is more suitable for EM-MWD short data transmission. When the bit error probability is  $10^{-6}$ , the SNR of soft decision decoding is 5.2dB, which is better than the 8.3dB of hard decision decoding. With soft decision decoding, the coding gain of the BCH code (31,16) is 5.5dB and the bandwidth extension is 93.8%. BCH code (127,99) is more suitable for EM-MWD long data transmission. When the bit error probability is  $10^{-6}$ , the SNR of soft decision decoding is 5.9dB, which is better than the 7.0dB of hard decision decoding. With soft decision decoding, the coding gain of the BCH code (127,99) is 4.7dB and the bandwidth extension is 28.3%. Finally, the field tests show that compared with BPSK without BCH coding, the proposed BPSK-based BCH coding and modulation technology can reduce the decoding error rate by about 10 times in the extreme case of low SNR. When the SNR is relatively low, reliable communication conditions can still be achieved and the received data can be stabilized.

In the practical EM-MWD process, the depth of the well is different, and the amplitude of the receiver signal is also different. The amplitude of the received signal has a certain relationship with the depth of the transmission. Theoretically, the deeper the depth, the smaller the received signal amplitude. On the other hand, the amplitude of the received signal is also related to the resistivity of the formation and the properties of the drilling fluid. At the same time, the contact condition between the downhole instrument and the borehole wall will also cause the received signal to change. According to the simulations and experiments in this paper, the proposed BPSK-based BCH coding and modulation technology can obtain a certain coding gain compared with the uncoded BPSK system, reducing the system's error rate effectively.

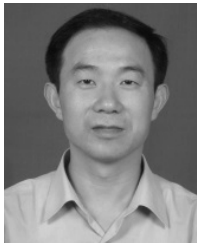
## REFERENCES

- [1] W. K. Han, L. S. Kumar, Y. L. Guan, and S. Sun, "Design of coded digital telemetry system for acoustic downhole channel with drilling noise," in *Proc. 9th Int. Conf. Inf., Commun. Signal Process.*, Dec. 2013, pp. 1–5.
- [2] Z. C. Qiao, L. X. Tang, and H. Liu, "Adaptive filtering algorithm for cancelling the pump noise in the mud pulse signal," *Chin. J. Sci. Instrum.*, vol. 37, no. 7, pp. 1477–1484, 2016.
- [3] Y.-T. Shao, A.-G. Yao, and M.-G. Zhang, "Application and development of electro-magnetic telemetry in drilling operation," *Coal Geol. Explor.*, vol. 35, no. 3, pp. 77–80, 2007.
- [4] Y. Yao, X. Ju, J. Lu, and B. Men, "Acoustic emission and echo signal compensation techniques applied to an ultrasonic logging-while-drilling caliper," *Sensors*, vol. 17, no. 6, p. 1351, 2017.
- [5] S. M. S. Moosavi, B. Moaveni, B. Moshiri, and M. R. Arvan, "Auto-calibration and fault detection and isolation of skewed redundant accelerometers in measurement while drilling systems," *Sensors*, vol. 18, no. 3, p. 702, 2018.
- [6] X. Li, A. Yao, and Y. Li, "Transmission characteristics of new electromagnetic-measurement while drilling system," *Coal Geol. Explor.*, vol. 38, no. 2, pp. 22–25 and 94, 2010.
- [7] H. Liu, H. Dong, Z. Liu, J. Ge, B. Bai, and C. Zhang, "Noise characterization for the FID signal from proton precession magnetometer," *J. Instrum.*, vol. 12, Jul. 2017, Art. no. P07019.
- [8] M. Y. Xia and Z. Y. Chen, "Attenuation predictions at extremely low frequencies for measurement-while-drilling electromagnetic telemetry system," *IEEE Trans. Geosci. Remote Sens.*, vol. 31, no. 6, pp. 1222–1228, Nov. 1993.
- [9] J. Schnitger and J. D. Macpherson, "Signal attenuation for electromagnetic telemetry systems," in *Proc. SPE/IADC Drilling Conf. Exhib.* Amsterdam, The Netherlands: Society of Petroleum Engineers, Mar. 2009, p. 118872.
- [10] Y. H. Fan, Z. P. Nie, and T. L. Li, "EM channel theory model and characteristics analysis for MWD," *Chin. J. Radio Sci.*, vol. 28, no. 5, pp. 909–914, 2013.
- [11] J.-H. Wang, H.-B. Dong, and Z.-J. Shi, "Modeling an EM channel for MWD in underground coal mine," *J. China Coal Soc.*, vol. 40, no. 7, pp. 1705–1710, 2015.
- [12] L. Xu, J. Chen, Z. Cao, X. Liu, and J. Hu, "Manchester code telemetry system for well logging using quasi-parallel inductive-capacitive resonance," *Rev. Sci. Instrum.*, vol. 85, no. 7, pp. 074704-1–074704-10, 2014.
- [13] C. Wei, J. Peipei, G. Qingshui, and Z. Songwei, "A trellis coded pulse interval modulation for measurement while drilling telemetry," in *Proc. IEEE 11th Conf. Ind. Electron. Appl. (ICIEA)*, Jun. 2016, pp. 522–525.
- [14] S. Reyes, R. Hutin, R. W. Tennent, and C. P. Reed, "Mud pulse telemetry data modulation technique," U.S. Patent 8 302 685 B2, Nov. 6, 2012.
- [15] B. Tu et al., "Research on MWD mud pulse signal extraction algorithm based on PLM encoding," *J. Electron. Meas. Instrum.*, vol. 2, pp. 227–232, Aug. 2015.
- [16] Y. Ningping, Z. Jie, J. Xing, and H. Hanjing, "Status and development of directional drilling technology in coal mine," *Procedia Eng.*, vol. 73, pp. 289–298, Jun. 2014.
- [17] M. Li, J. P. McGeehan, and A. Bateman, "Theoretical performance comparison between reference-based coherent BPSK and BCH coded differential BPSK," in *Proc. Commun. Global Users (GLOBECOM)*, Dec. 1992, pp. 1791–1796.
- [18] W. R. Gardner, V. V. Shah, and C. A. Robbins, "Acoustic telemetry system using passband equalization," U.S. Patent 8 634 273 B2, Jan. 21, 2014.
- [19] K. Liu, W. Lishuang, and S. Chaohui, "The development and application of Model CEM-1 electromagnetic measuring while drilling system," *China Petroleum Machinery*, vol. 40, no. 2, pp. 11–14, 92, and 98, 2012.
- [20] L. Long, Q. Chen, and F. Liu, "Research on eliminating interference signal algorithm of EM-MWD," *Chin. J. Sci. Instrum.*, vol. 35, no. 9, pp. 2144–2152, 2014.
- [21] G. A. Hassan and P. L. Kurkoski, "Zero latency image compression for real time logging while drilling applications," in *Proc. MTS/IEEE OCEANS*, Sep. 2005, pp. 191–196.
- [22] J. Li, "Unequal error protection for embedded coding of borehole images and variable-quality telemetry channels," U.S. Patent 8 694 870 B2, Apr. 8, 2014.
- [23] W. M. Savage, *Wellbore Communication, Downhole Module, and Method for Communicating*, U.S. Patent 8 358 220 B2, Jan. 22, 2013.
- [24] R. Mehra, G. Saini, and S. Singh, "FPGA based high speed BCH encoder for wireless communication applications," in *Proc. IEEE Int. Conf. Commun. Syst. Netw. Technol.*, Jun. 2011, pp. 576–579.
- [25] Y. Lee, H. Yoo, I. Yoo, and I.-C. Park, "High-throughput and low-complexity BCH decoding architecture for solid-state drives," *IEEE Trans. Very Large Scale Integr. (VLSI) Syst.*, vol. 22, no. 5, pp. 1183–1187, May 2014.

- [26] J. Spinner *et al.*, "A BCH decoding architecture with mixed parallelization degrees for flash controller applications," in *Proc. IEEE Int. SOC Conf. (SOCC)*, Sep. 2013, pp. 116–121.
- [27] J. G. Proakis and M. Salehi, *Digital Communications*. New York, NY, USA: McGraw-Hill, 2008.
- [28] S. Lin and D. J. Costello, *Error Control Coding*. New Delhi India: Pearson, 2001.
- [29] J. R. Wait and D. A. Hill, "Theory of transmission of electromagnetic waves along a drill rod in conducting rock," *IEEE Trans. Geosci. Electron.*, vol. GE-17, no. 2, pp. 21–24, Apr. 1979.
- [30] P. DeGauque and R. Grudzinski, "Propagation of electromagnetic waves along a drillstring of finite conductivity," *SPE Drilling Eng.*, vol. 2, no. 2, pp. 127–134, 1987.



**CHENG ZHANG** received the M.S. degree in instrument science and technology from the China University of Geosciences, Wuhan, China, in 2015, where he is currently pursuing the Ph.D. degree in control science and engineering with the School of Automation. He has been involved in developing intelligent geophysical instruments, especially the electromagnetic measurement while drilling system. His current research interests include weak signal detection and intelligent geophysical instrument.

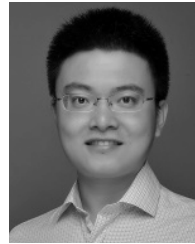


signal detection and intelligent geophysical instrument.

**HAOBIN DONG** received the Ph.D. degree from the Huazhong University of Science and Technology, China, in 2002. He was a Visiting Associate Professor with the Well Logging Laboratory and the Subsurface Sensing Laboratory, Department of Electrical and Computer Engineering, University of Houston, TX, USA, from 2005 to 2006. He is currently a Professor with the School of Automation, China University of Geosciences, Wuhan, China. His current research interests include weak



**JIAHAO WANG** received the Ph.D. degree in geodetection and information technology from the China University of Geosciences, Wuhan, China, in 2015, where he is currently a Lecturer with the School of Mechanical Engineering and Electronic Information. His current research interests include channel coding and telemetry instrument while drilling.



**JIAN GE** received the Ph.D. degree in geodetection and information technology from the China University of Geosciences, Wuhan, China, in 2014, where he is currently an Associate Professor with the School of Automation. He has developed a land and marine proton precession magnetic sensor based on pre-polarization and dynamic nuclear polarization effect, a landmine detector, and an unexploded ordnance detector. His current research interests include weak signal detection and geophysical detection method and instrument.



**HUAN LIU** (S'15–M'18) received the Ph.D. degree in geodetection and information technology from the Institute of Geophysics and Geomatics, China University of Geosciences, Wuhan, China, in 2018, where he is currently an Associate Professor with the School of Automation. From 2016 to 2017, he was a joint training Ph.D. Student in electrical engineering and computer science with the School of Engineering, The University of British Columbia, Kelowna, Canada. He has been involved in developing intelligent geophysical instruments, especially the proton magnetometer and the Overhauser magnetometer. His current research interests include weak magnetic detection, signal processing, data mining, and machine learning.

**ZHIWEN YUAN** is currently a Senior Engineer of the Science and Technology on Near-Surface Detection Laboratory, Wuxi, China. His current research interest includes near-surface detection technology.

**JUN ZHU** is currently an Engineer of the Science and Technology on Near-Surface Detection Laboratory, Wuxi, China. His current research interest includes near-surface detection technology.

**HAIYANG ZHANG** is currently an Engineer of the Science and Technology on Near-Surface Detection Laboratory, Wuxi, China. His current research interest includes near-surface detection technology.

...